On the Pressure Balance and Plasma Transport in Cylindrical Magnetized Arcs

D. C. Schram, I. J. A. M. v. d. Mullen, B. F. M. Pots *, and C. J. Timmermans

Eindhoven University of Technology, The Netherlands

Magnetized current-carrying plasmas exhibit usually significant $E \times B$ rotation velocities which often approach the ion thermal velocity. It is shown both experimentally and theoretically that this rotation in combination with inertia, viscosity and friction leads to an important reduction of the radial transport. If the radial electric field component is directed inward an inwardly directed force on the ions is set up. On the other hand, turbulence leads to enhanced transport especially at higher values of the electron Hall parameter. Also this effect is observed in this experiment and is shown to be in accordance with measured turbulence levels.

1. Introduction

In the past several investigations have been conducted to explain the observed pressure enhancement in magnetized arcs (cf. e.g. refs. [1 – 4]). The role of the magnetic field is to reduce the electron heat conduction transverse to the magnetic field which results in a higher temperature at the axis of the discharge. Also the radial diffusion of particles is reduced, which on its turn results in a higher local pressure. In subsequent investigations the influence of B through the Nernsteffect was stressed [5 – 7]; in the presence of a negative radial temperature gradient an inwardly directed force is set up as a consequence of friction of the azimuthally directed Nernst-current. This effect reduces further the particle diffusion.

In most of these treatments ion viscosity and elastic terms as ion-neutral friction have been neglected. However in cylindrical arcs rotation is an important effect and the rotation velocities may approach the ion thermal velocity. As a consequence ion inertia, ion viscosity, ion-neutral friction, and finite particle sources may influence the transport significantly. Under certain conditions an important reduction of the ion radial velocity may occur. In other words, particle containment may be better than classical (including the pinch- and the Nernst-effects). As a consequence the pressure enhancement may also be enlarged by ion viscosity and ion-neutral friction.

In later publications [8, 9] the importance of rotation was realized. Klüber [8] calculated the potential distribution for *homogeneous* cylindrical arcs including the effect of ion viscosity. The rotational velocity was calculated from the potential distribution. Klüber obtained a good qualitative agreement with experimental observations (and the agreement would have even been better had the actual value for the axial conductivity been used). This in spite of the fact that some of the assumptions (zero radial component of ion drift velocity) are liable to criticism [10, 11], or do not apply to most experimental situations (homogeneity, no particle sources).

In a careful study of the mass balance for one particular discharge parameter set of a hollow cathode arc, Van der Mullen [13] showed that the measured particle diffusion, deduced from the mass source, was much smaller than predicted from classical theory. He could only obtain a rough agreement between measured source term and calculated transport if he included ion inertia, ion-viscosity and ion-neutral friction. In fact, for this specific experimental condition, the radial outflow of particles was so much reduced that it was reasonable to neglect the radial ion velocity, herewith justifying a posteriori one of Klübers' assumptions.

This evidence justified a careful examination of the nature of particle transport and the influence of plasma rotation. In this paper we will first recall the standard MHD-description of plasma transport including ion inertia, ion viscosity and ion-neutral friction. The results of these calculations will then

---

* At present Koninklijke Shell Laboratories, Amsterdam, The Netherlands.

Reprint requests to Prof. Dr. D. C. Schram, Eindhoven University of Technology, Den Dolech 2, 5600 MB Eindhoven.

be compared with experimental information on particle transport. Finally, the effect of turbulence on the transport will be indicated.

2. The Momentum Equations and Particle Transport

We consider the pressure balance of a strongly magnetized, current carrying plasma and assume that the electron Hall-parameter $\Omega_e \tau_{ei}$ is much larger than 1. Here Ω_e is the electroncyclotronfrequency and τ_{ei} is the electron-ion collision time for momentum transfer [14]:

$$\Omega_e \tau_{ei} \gg 1 \,. \tag{1}$$

Only under this condition the radially directed electron heat conduction will be largely reduced. Also we deal with elongated plasmas; the axial gradients (characterized by $1/L$) are much weaker than radial gradients (characterized by $1/\Lambda$):

$$L/\Lambda \gg 1 \,. \tag{2}$$

In this paper we will assume throughout that the plasma is singly ionized ($Z = 1$) and that only one type of ion is present. Quasi-neutrality requires the electron density, n_e, to be equal to the ion density, n_i. The magnetic field is homogeneous and directed along the z-axis. Next, we consider only plasmas for which Coulomb interactions dominate over collisions of charged particles with neutrals:

$$\tau_{ea} \gg \tau_{ei} \,; \qquad \tau_{ia} \gg \tau_{ii} \,. \tag{3}$$

Here τ_{ei} and τ_{ii} are the characteristic collision times for e-i and i-i interactions as given by Braginskii [14] and τ_{ea} and τ_{ia} are the characteristic times for electron neutral and ion-neutral interactions respectively. For relatively cool "radiative" plasmas with temperatures in the few eV-range both inequalities (3) are already fulfilled for relatively low ionization degrees: $n_e/(n_e + n_a) > 0.1$; n_a is the neutral density. This condition is a reasonable good guide for most types of (cool) plasmas (independent of the type gas and the plasma density, etc.) and will be met even in the periphery of magnetized cylindrical arcs. The assumptions (3) indicate that Coulomb interactions dominate the deformation of the velocity distribution and in the MHD-ordering we are entitled to use Braginskii's transport coëfficients throughout. A second consequence of (3) is that we may neglect the electron neutral friction $\boldsymbol{R}^{ea}$ with respect to the electron-ion friction $\boldsymbol{R}^{ie} = - \boldsymbol{R}^{ei}$.

For the MHD-theory to be valid we must assume that the radial dimension Λ is much larger than the smallest of ϱ_i (ion cyclotron radius) and λ_{ii} (the mean free path for ion-ion collisions)

$$\begin{aligned} \lambda_{ii}/\Lambda \ll 1 \quad &\text{for} \quad \Omega_i \tau_i \lesssim 1 \,, \\ \varrho_i/\Lambda \ll 1 \quad &\text{for} \quad \Omega_i \tau_{ii} \gtrsim 1 \,. \end{aligned} \tag{4}$$

The ion Hall parameter $\Omega_i \tau_{ii}$ may take values below and above unity. Most of the experimental evidence in this paper relates to unmagnetized ions: $\Omega_i \tau_{ii} \lesssim 1$.

As the electron cyclotron radius ϱ_e is usually much smaller than ϱ_i the condition $\varrho_e/\Lambda \ll 1$ is in general an automatic consequence of (4). In the MHD-ordering only the azimuthal $\boldsymbol{E} \times \boldsymbol{B}/B^2$ velocity may be of the order of the ion thermal velocity $v_{thi} = (2kT_i/M_i)$; the ion diamagnetic drift velocity $w_{di} = \nabla p_i/n_e e B_z$ must be smaller than v_{thi}. Therefore, the rotational drift velocities of electrons and ions, $w_{\theta e}$ and $w_{\theta i}$ (which are both mainly of $\boldsymbol{E} \times \boldsymbol{B}$-origin and are comparable in magnitude) may reach the *ion* thermal velocity v_{thi}, but will remain small compared to v_{the}. So, all components of the drift velocities $\boldsymbol{w}_e$ and $\boldsymbol{w}_i$ except $w_{\theta i}$ are small compared to their respective thermal velocities:

$$\begin{aligned} \frac{w_{\theta i}}{v_{thi}} \lesssim 1 \,; \quad &\frac{w_{ri}}{v_{thi}} \ll 1 \,; \quad \frac{w_{zi}}{v_{thi}} \ll 1 \,; \\ \frac{w_{\theta e}}{v_{the}} \ll 1 \,; \quad &\frac{w_{re}}{v_{the}} \ll 1 \,; \quad \frac{w_{ze}}{v_{the}} \ll 1 \,. \end{aligned} \tag{5}$$

As a consequence we may neglect electron inertia, electron viscosity and electron-neutral friction, while we must retain ion inertia, ion viscosity and ion-neutral friction in the momentum equations. In the stationary state we obtain from usual MHD-theory (e.g. Braginskii [14]) the following equations for the momentum balances:

$$\begin{aligned} n_i m_i (\boldsymbol{w}_i \cdot \nabla) \, \boldsymbol{w}_i + \nabla p_i + \nabla \cdot \boldsymbol{\Pi}_i \\ = + e \, n_i (\boldsymbol{E} + \boldsymbol{w}_i \times \boldsymbol{B}) - \boldsymbol{R}^{ie} - \boldsymbol{R}^{ia} - \boldsymbol{M}^{Si} \,, \quad (6) \\ \nabla p_e = - e \, n_e (\boldsymbol{E} + \boldsymbol{w}_e \times \boldsymbol{B}) + \boldsymbol{R}^{ie} - \boldsymbol{M}^{Se} \,. \end{aligned}$$

Here $\boldsymbol{M}^{Si}$ and $\boldsymbol{M}^{Se}$ represent the source contributions to these equations, i.e. the momentum loss associated with finite sources:

$$\begin{aligned} \boldsymbol{M}^{Si} &= n_i m_i (\boldsymbol{w}_i - \boldsymbol{w}_a) \, v_{ion} \,; \\ \boldsymbol{M}^{Se} &= n_e m_e (\boldsymbol{w}_e - \boldsymbol{w}_a) \, v_{ion} \,; \end{aligned} \tag{7}$$

where v_{ion} refers to the ionization frequency. As we deal with singly ionized ions, charge neutrality requires $n_i = n_e = n$.

Usually, plasmas which satisfy the conditions (3) do meet also a supplementary condition: $\tau_{\text{ion}} = 1/\nu_{\text{ion}} \gg \tau_{\text{ei}}$ (3). Under these conditions also the source contribution M^{Se} can be neglected with respect to R^{ei}.

With the introduction of mass velocity w_m and current density j:

$$w_m = \frac{m_i w_i + m_e w_e}{m_i + m_e}; \quad j = ne(w_i - w_e), \quad (8)$$

we can transform the momentum equations into two macroscopic equations, viz., Ohms law:

$$E + w_m \times B = \frac{j \times B}{n_e e} + \frac{R^{ie}}{n_e e} - \frac{\nabla p_e}{n_e e}, \quad (9)$$

Navier Stokes equation:

$$j \times B - \nabla (p_e + p_i)$$
$$= \nabla \cdot \boldsymbol{\Pi}_i + n_i m_i (w_i \cdot \nabla) w_i + R^{ia} + M^{\text{Si}}. \quad (10)$$

Several important differences with the usual MHD-description become evident from Ohms law and Navier Stokes equation:

1. Since $j \times B \neq \nabla p$, a radial component of the current density may exist as a consequence of ion rotation (through ion-inertia, ion viscosity and ion-neutral friction). The diffusion does not need to be ambipolar in the presence of rotation.

2. As there is radial current there must be also an axial dependence of j_z (since $\nabla \cdot j = 0$). Apparently, in the presence of rotation there exist weak axial gradients; strictly speaking, cylindrical symmetry is not valid for magnetized arcs.

3. Ion rotation may give rise to additional pressure enhancement (see Equation 10).

3. Radial Transport in the Quasi-Cylindrical Case

The radial and azimuthal components of the ion- and electron-momentum equations are starting

points of our discussion; z-direction is along the applied magnetic field, $B_z = B_0$. The radial components are (R_r^{ie} is very small and is ignored):

$$- n_i m_i \frac{w_{\theta i}^2}{r} = n_i e E_r + n_i e w_{\theta i} B_z$$
$$- \frac{\partial p_i}{\partial r} - (\nabla \cdot \boldsymbol{\Pi}_i) - R_r^{ia} - M_r^{\text{Si}} \quad (11)$$

$$0 = - n_e e E_r - n_e e w_{0e} B_z - \frac{\partial p_e}{\partial r} - j_z B_0 \quad (12)$$

where it is assumed that $|w_{zi}| \ll |w_{ze}|$. The contributions of ion viscosity, ion-inertia and ion neutral friction have been investigated for both the regimes of unmagnetized ions ($\Omega_i \tau_{ii} < 1$) and magnetized ions ($\Omega_i \tau_{ii} > 1$) for the ordering given by inequalities (1), (2), (3), (4), (5). The leading term of the r-component of the viscosity

$$(\nabla \cdot \boldsymbol{\Pi}_i)_r \cong - \left[2 \eta_3 \frac{\partial}{\partial r} \left(\frac{w_{0i}}{r} \right) + \frac{\partial}{\partial r} \eta_3 r \frac{\partial}{\partial r} \left(\frac{w_{0i}}{r} \right) \right] \quad (13)$$

is small compared to $\partial p_i / \partial r$ for both regimes. In App. A the viscosity coefficients are given. The dominant term of the r-component of the ion-inertia $n_i m_i (w_{0i}^2/r)$ can be of the same order as $\partial p_i / \partial r$ in the unmagnetized ion regime; for $\Omega_i \tau_{ii} > 1$ it can be neglected.

Finally, the radial components of ion-neutral friction and source contribution can be neglected with respect to $\partial p_i / \partial r$ for both regimes. Adding (11) and (12) and making use of the simplifications which are valid for both regimes, we find (with $n_e = n_i = n$):

$$j_0 B_z = - n m_i \frac{w_{0i}^2}{r} + \frac{\partial (p_e + p_i)}{\partial r} + j_z B_0. \quad (14)$$

If we insert this expression in the θ-component of the ion-momentum equation:

$$n m_i \left[\frac{w_{ri}}{r} \frac{\partial}{\partial r} (r w_{0i}) + w_{zi} \frac{\partial w_{0i}}{\partial z} \right] = - n e w_{ri} B_z - (\nabla \cdot \boldsymbol{\Pi}_i)_0 - \frac{e n j_0}{\sigma_\perp} + \frac{3}{2} \frac{n}{\Omega_e \tau_{ei}} \frac{\partial k T_e}{\partial r} - R_0^{ia} - M_0^{\text{Si}} \quad (15)$$

and solve the expression for $n w_{ri}$, we obtain with $\sigma_\perp = n e^2 \tau_{ei}/m_e$:

$$n w_{ri} = \frac{1}{\Omega_e \tau_{ei} e B_z \left(1 + \underbrace{\frac{1}{\Omega_i r} \frac{\partial}{\partial r} r w_{0i}}_{\text{inertia}} \right)}$$
$$\times \left[\left\{ \underbrace{n m_i \frac{w_{0i}^2}{r}}_{\text{inertia}} - \underbrace{\frac{\partial (p_e + p_i)}{\partial r}}_{\text{classical}} + \underbrace{\frac{3}{2} n \frac{\partial k T_e}{\partial r}}_{\text{Nernst}} - \underbrace{j_z B_0}_{\text{pinch}} \right\} - \Omega_e \tau_{ei} \{ \underbrace{(\nabla \cdot \boldsymbol{\Pi}_i)_0}_{\text{viscosity}} + \underbrace{R_0^{ia}}_{\text{friction}} + \underbrace{M_0^{\text{Si}}}_{\text{source}} \} \right]. \quad (16)$$

Here the axial component of the inertial term is neglected. Several conclusions follow from comparison of this relation with the "classical" expression for zero rotation; "classical" stands for classical transport including the Nernst- and the pinch-terms:

$$(n\,w_{\mathrm{ri}})_{\mathrm{class}} = \frac{-1}{\Omega_\mathrm{e}\,\tau_{\mathrm{ei}}\,e B_z}\left[\frac{\partial\,(p_\mathrm{e}+p_\mathrm{i})}{\partial r} - \frac{3}{2}\,n\,\frac{\partial k T_\mathrm{e}}{\partial r} + j_z\,B_\theta\right], \tag{17}$$

The following comments can be made:

a) The expression (16) for radial transport contains two terms:

1. The first is quite similar to the "classical" expression apart from two corrections (one in the nominator and one in the denominator both from inertia). These corrections may be of order 1 for $\Omega_\mathrm{i}\,\tau_{\mathrm{ii}} < 1$, but can be ignored for $\Omega_\mathrm{i}\,\tau_{\mathrm{ii}} > 1$. We will denote this term by the quasi-classical contribution to the transport.

2. The second term is related to the rotation and will be called the rotational contribution. This term is magnified by $\Omega_\mathrm{e}\,\tau_{\mathrm{ei}}$ and can not be neglected in many cases especially for conditions with significant rotation.

b) Since $\Omega_\mathrm{e}\,\tau_{\mathrm{ei}} \gg 1$ the rotational part of $n\,w_{\mathrm{ri}}$ can be easily as large as the quasi-classical contribution. The direction of the ion-flux depends on the sign of $w_{\theta i}$ and thus on the sign of E_r (more precisely, on the sign of $E_\mathrm{r} - \frac{1}{n\,e}\frac{\partial p_\mathrm{i}}{\partial r}$ see (11)). If $E_\mathrm{r} < 0$, i.e. $\boldsymbol{E}$ is directed inward (positive rotation) the flux is also directed inwards; in other words the diffusion is reduced, if $E_\mathrm{r} > 0$ (negative rotation) the rotational contribution to the flux is directed outwards, i.e. transport is enhanced (cf. Figure 1). The detailed potential distribution depends on the geometry and the location of the electrodes [8, 9]; one finds in general that $E_\mathrm{r} < 0$ (and thus transport reduction) at the cathode side and $E_\mathrm{r} \gtrsim 0$ (and thus enhancement of transport) at the anode side.

In the present experimental arrangement the anode radius is substantially larger than the cathode radius, Figure 1 a I. Then the radial electric field is directed inward for a long part of the arc and consequently ion transport is reduced. Close to the anode still a reversal of ion rotation may occur [12, 23], but the neutral point (no rotation) is close to the anode as is sketched in Figure 1 b I.

In symmetrical anode-cathode arrangement Fig. 1 a II as used in [7, 8], we would find again a positive rotation of the cathode side and negative rotation at the anode side. But now the negative rotation at anode side is much more extended and a neutral rotation point is expected to occur roughly halfway anode-cathode, Figure 1 b II.

The experimental results reported in this paper are obtained in the asymmetrical arrangement as sketched in Fig. 1 a I at a position halfway cathode-anode. The theoretical treatment is general and can also be applied to other geometries with appropriate changes for the axial dependence of the ion rotational profile.

As an additional confinement occurs at cathode side and a additional transport at anode side one must expect a z-dependence of the plasma parameters even in geometrically cylindrical arcs. Axial inhomogeneity, though weak, is an essential feature of magnetized arcs.
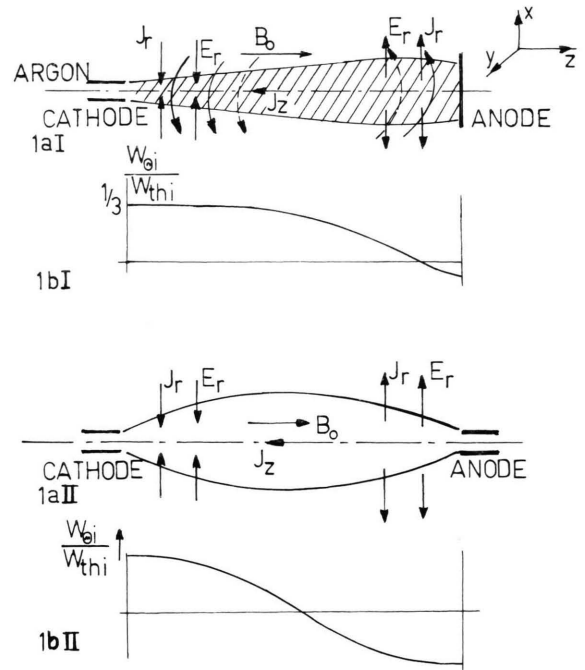

Fig. 1. a) Sketch of the radial electric field and current density in a magnetized arc, for asymmetric (I) and symmetric (II) cathode-configurations. b) Sketch of the maximum rotation velocity normalized to the ion thermal velocity as a function of z.

c) From the θ-component of the electron momentum equation we can deduce:

$$n\,w_{\rm re} = -\frac{n\,j_\theta}{\sigma_\perp B_z} + \frac{3}{2}\,\frac{n}{\Omega_{\rm e}\tau_{\rm ei}\,e\,B_z}\,\frac{\partial k\,T_{\rm e}}{\partial r}\,. \quad (18)$$

It follows from comparison with (16), that the radial velocities are not equal; in other words a radial current is present, and the diffusion is not ambipolar.

The radial component of the current density is given by:

$$j_{\rm r}\,B_z = -\,n\,m_{\rm i}\left\{\frac{w_{\rm ri}}{r}\,\frac{\partial}{\partial r}\,(r\,w_{\theta{\rm i}}) + w_{z{\rm i}}\,\frac{\partial w_{\theta{\rm i}}}{\partial z}\right\} \\ -\,(\nabla\cdot\boldsymbol{\varPi}_{\rm i})_\theta - R_\theta^{\rm ia} - M_\theta^{\rm Si}\,. \quad (19)$$

All contributions contain linearly the rotational velocity $w_{\theta{\rm i}}$ and with the same sign; thus all terms add. A positive ion rotation, $w_{\theta{\rm i}} > 0$, gives rise to a negative radial component of the current density consistent with the rotational confinement of the ions, see (b). If the ion-neutral friction term $R_\theta^{\rm ia}$ and/or the similar source contribution term $M_\theta^{\rm Si}$ dominate then we may write

$$j_{\rm r}\,B_z = -R_\theta^{\rm ia} - M_\theta^{\rm Si} = -\,n\,m_{\rm i}(w_{\theta{\rm i}} - w_{\theta a})\,(v_{\rm ia} + v_{\rm ion})\,.$$

If $w_{\theta a} \ll w_{\theta{\rm i}}$ and $w_{\theta{\rm i}} \simeq -E_{\rm r}/B_z$, then we obtain:

$$j_{\rm r} = \frac{n\,m_{\rm i}\,E_{\rm r}(v_{\rm ia} + v_{\rm ion})}{B_z^2} = \sigma_{\rm r}\,E_{\rm r} \quad (20)$$

in which an apparent transverse (rotational) conductivity

$$\sigma_{\rm r} = \frac{n\,m_{\rm i}(v_{\rm ia} + v_{\rm ion})}{B_z^2} \quad (21)$$

appears. This expression is a generalized form of the result of Lehnert [9]; it contains in the present form also the particle source contribution.

d) From the law $\nabla\cdot\boldsymbol{j} = 0$ we can conclude immediately

$$\frac{\partial j_z}{\partial z} = -\frac{1}{r}\,\frac{\partial}{\partial r}\,r\,j_{\rm r} \neq 0\,. \quad (22)$$

Again, axial inhomogeneity proves to be an essential feature of magnetized arcs. However, in current carrying plasmas it requires only very small changes in the axial component of the current density (carried mostly by the electrons) to accommodate the required radial component of the current density. Though principally essential, the inhomogeneity of j_z can be ignored in most calculations.

4. The Comparison with Measured Diffusion and the Contribution of Viscisoty and Friction

We will investigate the effect of the rotational contribution to the radial transport by comparing the measured diffusion flow to the classical diffusion flow (17). This comparison is simplified by the fact that several contributions to the diffusion can be ignored for the conditions valid for the hollow cathode arc used for the study. The gradient of $T_{\rm e}$ is weaker than the gradient of $n_{\rm e}$. Further, $T_{\rm i}$ is smaller than $T_{\rm e}$ and $T_{\rm i}$ is constant over the radius; the ion inertia term which may approach the $\nabla p_{\rm i}$-term will also be smaller than the $k\,T_{\rm e}\,\partial n_{\rm e}/\partial r$ term. Then the Nernst term can be combined partly with the $\nabla p_{\rm e}$-term to $k\,T_{\rm e}\,\partial n_{\rm e}/\partial r$. Finally also the pinch-term can be neglected for the plasma under consideration, as the poloidal beta, the ratio between electron kinetic pressure and magnetic pressure of the poloidal field, is large: $\beta_{\theta{\rm e}} = 2\mu_0\,n_{\rm e}\,k\,T_{\rm e}/B_\theta^2(R) \gg 1$.

So, in our case the expression for the classical diffusion is in a good approximation

$$(n\,w_{\rm ri})_{\rm class} = \frac{-\,k\,T_{\rm e}}{\Omega_{\rm e}\,\tau_{\rm ei}\,e\,B_z}\,\frac{\partial n_{\rm e}}{\partial r} = -D^{\rm class}\,\frac{\partial n_{\rm e}}{\partial r} \quad (23)$$

where

$$D^{\rm class} = \frac{k\,T_{\rm e}}{\Omega_{\rm e}\,\tau_{\rm ei}\,e\,B_z} \quad (24)$$

is the well known classical diffusion coëfficient.

The total contribution of the ignored classical terms, of which some are positive and others negative, amounts to at maximum 30% of the leading term. The measured diffusion coëfficient, $D^{\rm meas}$, can be compared with the classical diffusion coëfficient. If $D^{\rm meas} < D^{\rm class}$ then this points to rotational confinement, if $D^{\rm meas} > D^{\rm class}$ then also anomalous diffusion is present.

The importance of rotational effects depend on the magnitude of the azimuthal component of the ion drift velocity, $w_{\theta{\rm i}}$. Formally, MHD-ordering requires that the maximum value of $w_{\theta{\rm i}}$ remains smaller than the thermal ion velocity $v_{\rm thi} \equiv \sqrt{2\,k\,T_{\rm i}/M_{\rm i}}$, which is independent of radius in our case:

$$\left(\frac{w_{\theta{\rm i}}}{v_{\rm thi}}\right)_{\rm max} = \alpha \lesssim 1\,. \quad (25)$$

If we assume in first order for the rotational frequency a Gaussian profile, which actually is ob-

served in experiments [15]:

$$\frac{w_{\theta i}}{r} = a_0 \, \Omega_i \, \exp - [r^2/\Lambda_\theta^2] \qquad (26)$$

then we obtain for a_0; see Appendix A2:

$$a_{0I} = \xi \, \frac{\varrho_i}{\Lambda_\theta}, \quad \text{with} \quad \xi = 2.33 \, \alpha \lesssim 1 \,. \qquad (27)$$

This scaling seems appropriate for small ion Hall parameters $\Omega_i \, \tau_i \ll 1$. This has been verified experimentally [15].

A second approach is, to assume that the azimuthal velocity is mainly of E/B origin. If also for the electrostatic potential a Gaussian profile is assumed:

$$\Phi(r) = \Phi_0 \exp(-r^2/\Lambda_\theta^2) \qquad (28)$$

then we obtain also a Gaussian profile for the rotational frequency:

$$\frac{w_{\theta i}}{r} = \frac{E_r}{r B_z} = -\frac{\partial \Phi/\partial r}{r B_z} = \frac{-2\,\Phi_0}{\Lambda_\theta^2 \, B_z} \exp(-r^2/\Lambda_\theta^2) \,. \qquad (29)$$

If we estimate Φ_0 to be equal to the electron temperature in Volt:

$$\Phi_0 = -\frac{k T_e}{e} \qquad (30)$$

then we obtain the following estimate for a_{0II}:

$$a_{0II} = \frac{2 k T_e}{e B_z \, \Omega_i \, \Lambda_\theta^2} = \frac{T_e}{T_i} \, \frac{\varrho_i^2}{\Lambda_\theta^2} \,. \qquad (31)$$

In the unmagnetized ion regime, $\Omega_i \, \tau_i \ll 1$, estimate II is not too much different from estimate I. For most of the conditions the ratio ϱ_i/Λ is close to 1. In the magnetized ion regime, estimate II may be more appropriate. As most of our experimental evidence pertains to unmagnetized ions, we will use (27) for estimating the magnitude of $w_{\theta i}$.

With (27) and Gaussian profiles for the rotational frequency and the density we obtain for the total transport for the central part of the plasma

$$n \, w_{ri} = -D_\perp \, \partial n/\partial r \qquad (32)$$

with a diffusion coefficient:

$$D_\perp = \frac{k(T_e + T_i) + \xi^2 k T_i - \Omega_e \tau_{ei} \xi k T_i \left(\dfrac{4 \lambda_{ii}}{\Lambda} + \dfrac{\Lambda(v_{io} + v_{ion})}{v_{thi}} \right)}{\Omega_e \tau_{ei} e B_z (1 + 2 \xi \varrho_i/\Lambda)} \,. \qquad (33)$$

Again, it is clear from the last term in (33) that the (negative) momentum source due to ionization plays formally a similar role as the ion-neutral momentum exchange. As ionization is a strong
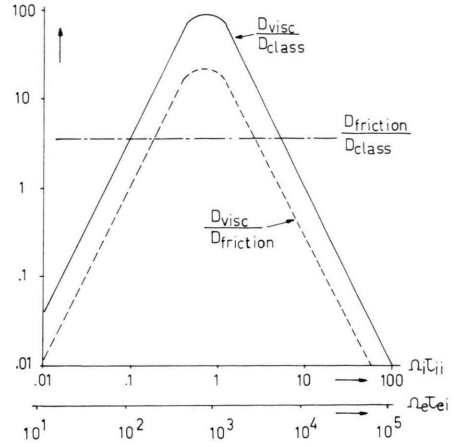

Fig. 2. Relative importance of various rotational contributions to radial ion transport as a function of the ion Hall parameter, see text.

function of the electron temperature and ion-neutral collisions depend very weakly on ion temperature it is clear that at low electron temperatures the ion-neutral momentum exchange dominates, while at high temperatures the ionization is more important.

The ratio $v_{thi}/(v_{ia} + v_{ion})$ can be represented as an effective mean free path for ion-neutral friction corrected for the additional effect of ionization. We will denote the quantity as $\lambda_{ia,s}$.

In deriving expression (33) we have neglected the pinch term and part of the Nernst-term but have retained the ion pressure term. If we ignore also these small terms in the numerator then we obtain:

$$D_\perp = \frac{\overbrace{k T_e}^{\text{classical}} - \Omega_e \tau_{ei} \xi k T_i \overbrace{\left(\dfrac{4 \lambda_{ii}}{\Lambda} + \dfrac{\Lambda}{\lambda_{ia,s}} \right)}^{\text{viscosity friction}}}{\Omega_e \tau_{ei} e B_z (1 + 2 \xi \varrho_i/\Lambda)} \,. \qquad (34)$$

Note, that the rotational contributions depend linearly on a_0, i.e. on the magnitude and the sign of $w_{\theta i}$. For the conditions of our experiment, E_r is directed inward ($E_r < 0$) and there is positive ion rotation ($a_0 > 0$). A strong reduction can be expected if either the viscosity or the friction term will become important. In fact, direct application of (34) with the estimate (27) for a_0 would even indicate "negative" diffusion for electron Hall parameter $\Omega_e \tau_{ei} > T_e \Lambda/T_i \, 4 \lambda_{ii} \sim 30$, while $\Omega_e \tau_{ei}$ can easily be

larger than 10^2. For these values of $\Omega_e \tau_{ei} > 10^2$ we find instead an anomalous enhancement of the transport. For low values of $\Omega_e \tau_{ei}$ we find indeed a significant reduction of the transport. Then the contribution of friction can also be significant. The ratio of the friction- (and source-) and ion viscosity contributions to the rotational confinement is ($\Omega_i \tau_{ii} < 1$):

$$\frac{R_\theta^{ia} + M_\theta^{Si}}{(\nabla \cdot \Pi_i)_\theta} = 4.4 \cdot 10^{-3} \left(\frac{\Lambda}{\lambda_{ii}}\right)^2 \left[\frac{n_a}{n_e} T_i^2 (\text{eV})\right] \left(1 + \frac{\langle \sigma \, v_e \rangle_{ion}}{\langle \sigma \, v_i \rangle_{ia}}\right). \tag{35}$$

If the ion energy balance can be reduced to a balance of ion heating by Coulomb-collisions and cooling by i-a friction plus transport then we may replace the term within square brackets by [0.25] as has been shown both theoretically and experimentally in [16, 17]. So for plasmas with small ion Hall parameters, for which λ_{ii}/Λ must be small compared to 1, the friction force can easily dominate the rotational confinement. For ion Hall parameters $\Omega_i \tau_{ii} > 1$, the viscosity contribution will become smaller with $(\Omega_i \tau_{ii})^2$, as the viscosity-coefficient η_1 decreases. For large ion Hall parameters (collisionless plasmas) the friction and source contributions may still be significant as compared to the very small classical confinement even for relatively low neutral densities. The situation is summarized in Fig. 2, for a temperature ratio $T_i/T_e = 1/3$, for

$$\left[\frac{n_a}{n_e} T_{i\,eV}^2\right] = 0.25 \text{ according to [17], and for } \frac{\varrho_i}{\Lambda} = \frac{1}{3} \text{ for } \Omega_i \tau_i \lesssim 1 \text{ and } \frac{\varrho_i}{\Lambda} = \frac{1}{3\Omega_i \tau_i} \text{ for } \Omega_i \tau_i > 1, \text{ and for argon.}$$

5. Pressure Enhancement

The rotational influence on the transport implies also a rotational influence on pressure enhancement in magnetized arcs [10, 18]. We can write:

$$\frac{\partial (p_e + p_i)}{\partial r} = \frac{3}{2} n \frac{\partial k T_e}{\partial r} - j_z B_\theta + n m_i \frac{w_{\theta i}^2}{r} - \Omega_e \tau_e \left[(\nabla \cdot \Pi^i)_\theta + R_\theta^{ia} + M_\theta^{Si} + n w_{ri} e B_z \left(1 + \frac{1}{\Omega_i r} \frac{\partial}{\partial r} r w_{\theta i}\right)\right]. \tag{36}$$

In earlier publications [5−6] the discussion was limited to the first two terms of the r.h.s. of (36). Special attention was paid to the contribution of the Nernst effect. However, (36) shows that rotational contributions and finite sources may also contribute significantly. Especially, if $E_r < 0$, positive rotation, rotational confinement may even dominate the pressure enhancement. Therefore, in our view it is not sufficient to test the Nernst-effect with the measured overall pressure enhancement [6, 7]; it is a much better test, to check the Nernst form of the (n_e, T_e) relation i.e. $n_e T_e^{-1/4} = \text{Ct.}$ for $Z_i = 1$ as a function of radius. In many cases the measured pressure enhancement can also be explained from rotational and source contributions. The contributions can be estimated by following the same procedure as in Section 4. Also here friction will contribute especially for low values of $\Omega_e \tau_{ei}$ and at the outer parts of the plasma where the neutral density will be large. For intermediate values of $\Omega_e \tau_{ei}$ viscosity would contribute significantly, but as stated we find then anomalous diffusion. Anomalous transport will of course limit the pressure built up and should be taken into account in the analysis.

6. Experimental Set Up and Procedure

For the verification of the transport model we used the Argon plasma of a Hollow Cathode Arc (HCA). The main characteristics are: applied magnetic field $B_z \leq 0.5$ Tesla; plasma current $I \leq 250$ A; pressure ≤ 0.5 Pascal; flow ≤ 10 cc NTP/sec; cathode diameter 10^{-2} m; the plasma length is 1.4 m. The measurements utilized in this paper are taken at the position halfway anode cathode: $z_0 = 0.75$ m. In Fig. 3 a sketch of the HCA is given. The plasma parameters are $10^{19}/\text{m}^3 < n_e < 2.10^{20}/\text{m}^3$; $2.5 < \hat{T}_e < 8$ eV, $1 < \hat{T}_i < 3$ eV. The plasma diameter will be slightly larger than the cathode diameter depending on the parameters n_e, T_e, B_0.

The plasmaparameters are measured with several diagnostics which are described extensively in [16, 17].

− n_e, T_e: Thomson scattering (50 J Ruby laser as source and a six-channels polychromator with a concave holographic grating) [19].

− T_i, T_a ⎱ Doppler width- and shift-measurements
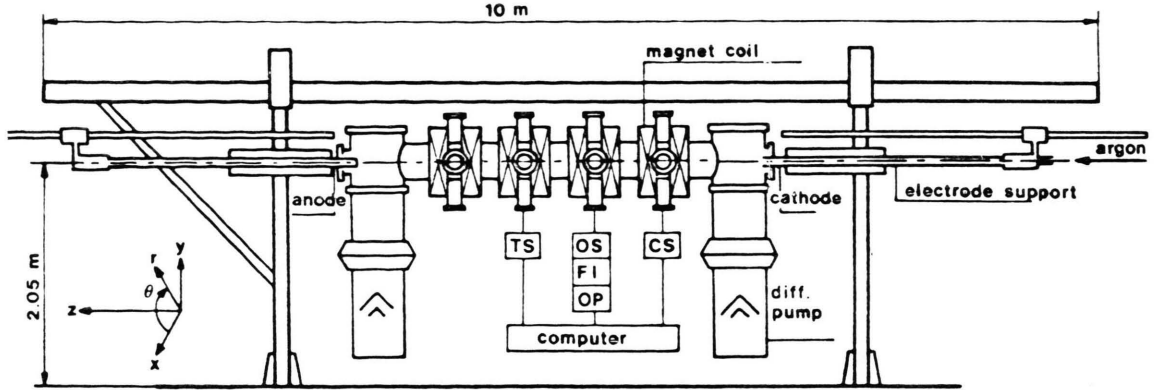 w_{0i}, w_{0a} ⎰ with a pressure scanned Fabry-Perot.

Fig. 3. Sketch of the hollow cathode discharge. TS = Thomson scattering diagnostic, OS = optical spectroscopy, FI = Fabry-Pérot interferometry, OP = optical probes, CS = collective scattering diagnostic.

— n_a: the neutral denisty n_a is determined from the ratio of excited level densities n_{4pI} and n_{4pII} of the 4 p groups in both the Ar I and Ar II systems (see Appendix B). Abel inversion is used to obtain the radial profiles of the level densities n_{4pI} and n_{4pII} (see [16]).

Before we describe results, we will outline the procedure to obtain the radial flow from the measured source term. From the ion mass-balance it follows that the divergence of the flow is equal to the mass-source term:

$$S_i \simeq n_e n_a \langle \sigma v_e \rangle_{ion} = \frac{1}{r} \frac{\partial}{\partial r} r n w_{ri} + \frac{\partial}{\partial z} n w_{zi} . \quad (37)$$

Though the axial flow velocities have been measured to be relatively large (up to $v_{thi}/10$) the axial gradients are weak and the divergence of the axial flow is small compared to the divergence of the radially directed flow. Recombination can be neglected for the considered parameter range and we obtain

$$(n w_{ri})_{exp} = \frac{1}{r} \int_0^r r' \, S_i(r') \, dr' \equiv - D^{exp} \frac{\partial n}{\partial r} . \quad (38)$$

From the measured values for n_e, n_a, T_e we can calculate the source and thus the actual radial flow $(n w_{ri})_{exp}$. This result can be compared with the theoretical expressions (33) and (34) derived in the preceding chapter.

We note that usually the axial contribution to the divergence of the *electron* flow $\partial n w_{ze}/\partial z$, can not be neglected. For current driven plasmas, the axial component of the electron drift may be large and even for the weak gradients the contribution of

$\partial n w_{ze}/\partial z$ may be appreciable. Since $j_r \neq 0$, $w_{er} \neq w_{ir}$; therefore we must calculate the *ion* radial flow as is indicated in (32) and is done in (38).

7. Fluctuations and Anomalous Transport

It will be shown in section 8 that for large $\Omega_e \tau_{ei}$ the diffusion is anomalously enhanced by the turbulence. Therefore, we have measured the fluctuation levels and the dispersions of the dominant types of instabilities. As diagnostics we used optical probing for the low frequency domain (< 1 MHz, sensitivity
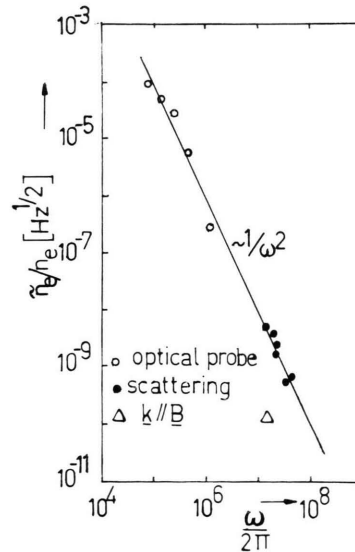

Fig. 4. Example of relative density fluctuation level as a function of the frequency. HCD parameter set: $I_{pl} = 100$ A, $B_z = 0.4$ T, $p_a = 0.5$ mTorr and $z = 0.25$ m

$\tilde{n}/n = 10^{-6}/\sqrt{Hz}$) and collective scattering of CO_2-laser light for higher frequencies [20].

For the present discussion only the low frequency (long wavelength) part of the spectrum is of importance as the spectral distribution follows a $1/\omega^2$-law as can be seen in Fig. 4 [20]. It appears both from collective scattering and from correlation of two optical probe signals, that the phase velocities of high frequency fluctuations (with frequencies f larger than the ion cyclotron frequency $\Omega_i/2\pi$) are around the ion acoustic velocity, c_s:

$$c_s \equiv \left(\frac{k T_e}{M_i} \right)^{1/2}. \tag{39}$$

We observe above the background $1/\omega^2$-spectrum definite instabilities:

— rotational instability

$$f < \Omega_i/2\pi, \, k_\perp \sim 1/R, \, k_{//} = 0 \,,$$

— drift instability

$$f \sim \Omega_i/2\pi, \, k_\perp \sim 1/R, \, k_{//} \sim 0 \,,$$

— ion-acoustic instability

$$f > \Omega_i/2\pi, \, k_\perp \sim \omega/c_s \,.$$

The first two instabilities may contribute to the anomalous transport. Of the third the level is too small to be significant. The rotational instability has been treated extensively in the literature; it is driven by velocity-shear and -gradients. It has large parallel wavelength ($k_{||} = 0$) and the azimuthal mode number is low: $m = 1$ or 2.

The instability can be treated as an excentric rotation of the plasmacolumn, cf. Figure 5. By optical probing we can estimate the modulation depth of the instability, which we define as $\delta = \Delta/\Lambda$, in which Δ is the excentricity and Λ is the radial Gaussian width of the intensity profile. As the emissivity of the plasma proves to be described by a Gaussian

$$\varepsilon_0(r) = \varepsilon_0 \exp\left[-y^2/\Lambda_\varepsilon^2 \right] \tag{40}$$

then we obtain for the lateral intensity profile:

$$I_0(y) = \sqrt{\pi} \, \varepsilon_0 \Lambda_\varepsilon \exp\left[-r^2/\Lambda_\varepsilon^2 \right] \tag{41}$$

and for the first harmonic at the frequency of the rotation instability:

$$I_1^{RMS}(y) = \frac{\Delta y \sqrt{2}}{\Lambda_\varepsilon^2} \, I_0(y) \,.$$

The maximum of $I_1(y)$ is $I_{1\,max}^{RMS}(y_{max}) = \varepsilon_0\sqrt{\pi} \, \Delta \exp(-\frac{1}{2})$ with $y_{max} = \Lambda/\sqrt{2}$, so we find:

$$\frac{\Delta}{\Lambda_\varepsilon} = \frac{I_{1\,max}^{RMS}(y_{max})}{I_0(0)} \exp(\tfrac{1}{2}) = \frac{I_{1\,max}^{RMS}}{I_0(y_{max})} \,. \tag{42}$$

Apparently, the modulation depth is equal to the ratio of the magnitude of the first harmonic to the D.C. value at $y = y_{max}$.

In Fig. 6 we have shown a measured profile for fluctuations with frequencies between 0 and 20 kHz, which contains both the first and second harmonic. This agrees reasonably with the calculated profile for Gaussian emissivity and $\Delta/\Lambda = 0.2$ if spatial integration due to the finite size of the probing beam has been taken into account. The residual measured signal in the centre of the discharge can be attributed to broadband drift waves. Though the typical frequencies of the driftwaves are higher, they may
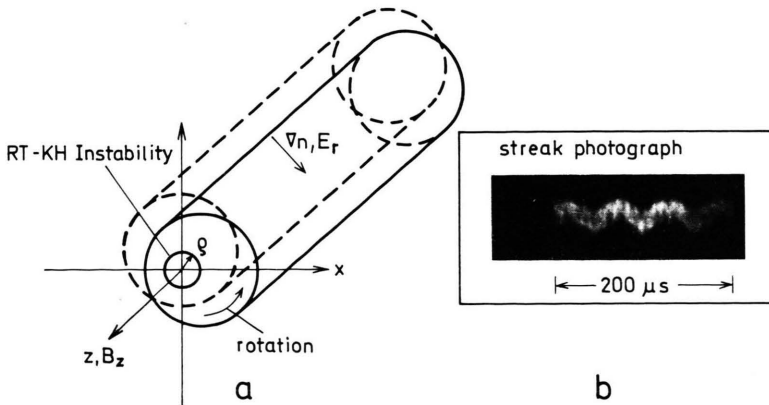

Fig. 5. a) Illustration of the rotational instability (Rayleigh-Taylor and Kelvin-Helmholtz). b) Streak photograph by Boeschoten et al. [12].
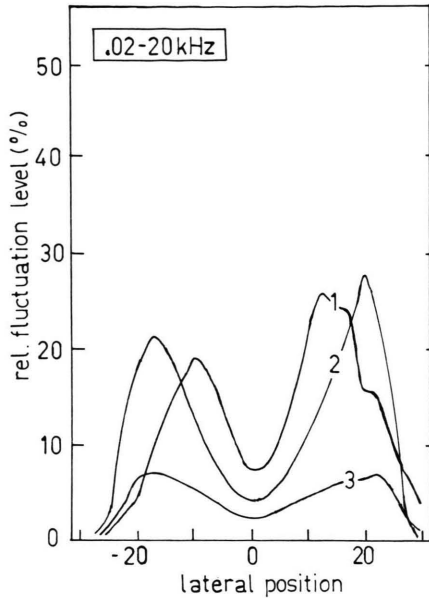
Fig. 6. Relative fluctuation level of fluctuations with frequencies up to 20 kHz as a function of the lateral position, y_0. Plasma parameters: $B_z = 2$ Tesla; $I = 30$ A (1), 120 A (2), 200 A (3), $Q = 8$ cm^3 NTP/s, $z = 0.75$ m.

contribute to lower frequencies. The levels in the driftwaves are of the order of 2% (cf. below) at the centre; because of this possible contribution the measured levels should be slightly reduced by a factor of 0.8.

The driftwaves have frequencies around the ion cyclotron frequency since $\varrho_i/\Lambda \sim 1$. If the pressure profile is also taken to be a Gaussian:

$$p(r) = p_0 \exp\left[-r^2/\Lambda^2\right]$$

then the fluctuations are expected to be localised around at $r = \Lambda/\sqrt{2}$. Both the presence of lower frequency rotational instability and the finite size of the probing beam flatten the lateral profile, cf. Figure 7. For the relative level we take here the local ratio of I_1^{RMS} and I_0. This of course is not entirely correct since an Abel inversion is required which would depend on the not a priori known azimuthal mode number. Taking the ratio may be a slight underestimate of the actual relative level.

Both the rotational and the drift instabilities may contribute to anomalous diffusion. For the rotational instability Janssen [21] derived the following expression for the diffusion coëfficient:

$$D_{an}^{(rot)} \simeq \left(\frac{\Delta}{\Lambda}\right)^3 \frac{k\,T_i}{e\,B}. \tag{43}$$

In the derivation it is assumed that there is a significant phase difference between the $\tilde{E}$-field and the density fluctuation $\tilde{n}_e(t)$. This phase difference is not measured, but the apparent nonlinearity of the phenomenon favours an important phase difference. On the other hand, the frequency spectrum is relatively small band, which suggest harmonic behaviour. Turbulence levels are given as functions of $\Omega_e\,\tau_{ei}$ in Figure 8.
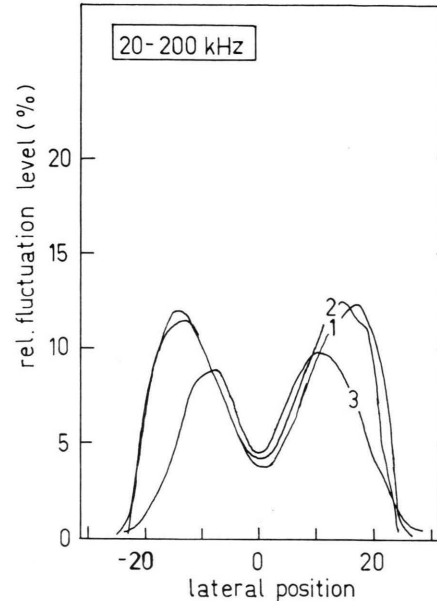

Fig. 7. Relative fluctuation level of drift fluctuations in the frequency domain 20 kHz – 200 kHz as a function of the lateral position. Same plasma conditions as in Figure 6.
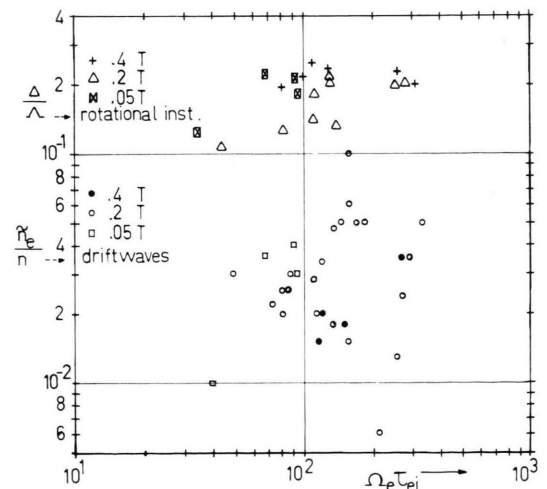

Fig. 8. Measured relative fluctuation levels for rotational and drift fluctuations as function of the electron Hall parameter.

The driftwaves are also observed to have low azimuthal wavenumbers: $m = 1$. They are localised around $r/\Lambda \sim 0.7$, but cover a relatively wide radial region. Therefore, we may estimate the turbulence on the basis of $k_\perp \Lambda \sim 1$ and from the maximum relative level (as function of y) The diffusion coëfficient is:

$$D_{\perp an}^{drift} \simeq \left(\frac{\tilde{n}_e}{n}\right)^2 \frac{kT_e}{eB_z}(k_\perp \Lambda). \qquad (44)$$

The driftwaves exhibit a broad spectral distribution. Therefore, it is reasonable to assume that there is a significantly phase difference between $\tilde{n}$ and $\tilde{\varphi}$. Also we find for all conditions $k_\perp \Lambda \sim 1$, as the mode number is $m = 1$ and the maximum level is observed close to the lateral position $y \simeq 0.7 \Lambda$.

The expressions (43) and (44) are of a similar functional form. If we compare the anomalous diffusion coëfficient with the classical diffusion coëfficient D_{class} then we obtain the well known estimate:

$$\frac{D_\perp^{turb}}{D_\perp^{class}} \simeq \left(\frac{\tilde{n}_e}{n}\right)^2 \Omega_e \tau_{ei}. \qquad (45)$$

We expect only a significant contribution to the diffusion by turbulence for larger values of the electron Hall parameter, also because the level of the driftwaves is observed to increase with $\Omega_e \tau_{ei}$.

8. Results and Discussion

Plasmaparameters and Diffusioncoëfficient

In Fig. 9. we show measured profiles of n_e and T_e as functions of radius r and axial position z are shown. In Fig. 10 measured profiles of the rotational velocities w_{0i}, w_{0a} are given. It is clear that the profile of $n_e(r)$ is more peaked than that of $T_e(r)$ as was assumed in section 4. Also the assumption of Gaussian profiles for the density and for the rotational frequency w_{0i}/r, appears to be realistic, see Figure 10.

For 40 experimental conditions we have measured n_e, T_e, T_i, T_a, p_a, n_a, w_{0i}/r, n_{4p}^I, n_{4p}^{II}, see [16, 17, 21] and values for $D_\perp^{class}$ and $D_\perp^{exp}$ for these parameter sets have been determined. For the calculation of the $D_\perp$ we have assumed Gaussian profiles which appears to be a realistic assumption. The profile widths Λ were determined from measured lateral profiles of 4p-4s Ar II-lines. We have re-
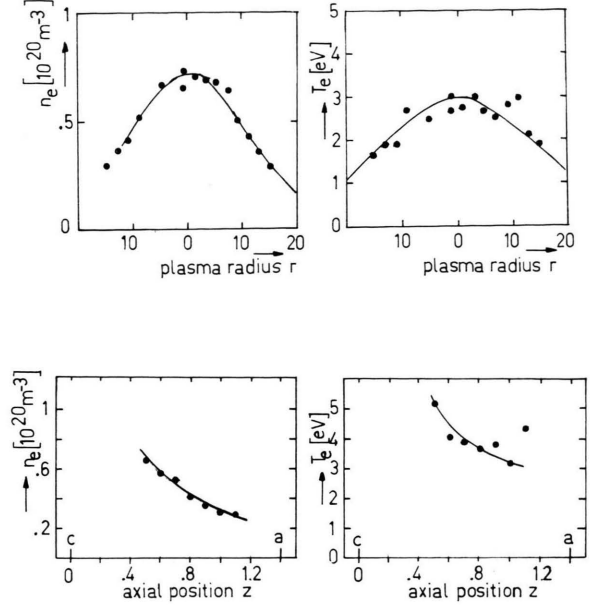

Fig. 9. The electron density n_e and the electron temperature T_e as functions of radius r and axial position z. Standard HCD parameters; flow $Q = 10$ cm³ NTP/s, $p_a \cong 2.5$ mTorr, $I = 50$ A, $z = 0.75$ m, $B = 0.2$ Tesla, $n_e = 7.2 \cdot 10^{19}/m^3$, $T_e = 2.8$ eV.
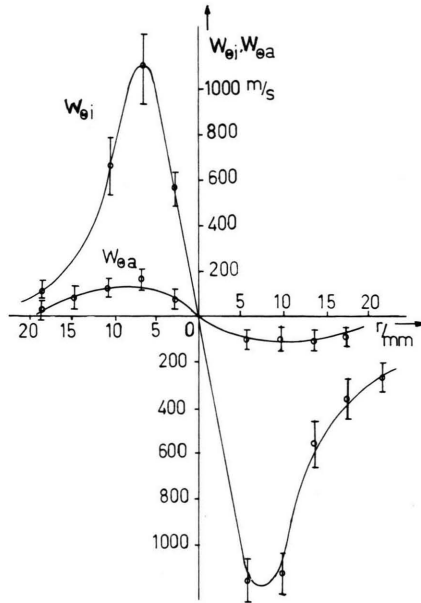

Fig. 10. Measured ion and neutral azimuthal velocities as a function of radius. Full curves represent Gaussian fits for the rotation frequencies w_0/r. $B = 0.2$ Tesla, $p_a = 2.5$ mTorr, $I = 50$ A, $Q = 9$ cm³ NTP/s, $z = 0.75$ m.

stricted the analysis to the central part of the plasma with radius $r < \Lambda$. As we are interested in the *average* transport for the central part of the plasma the sketched procedure will yield results with small uncertainties due to deviations of the exact gradients from Gaussians. We estimate these uncertainties at 30% based on comparisons with experimentally obtained profiles with the assumed Gaussians.

In Fig. 11 the so determined diffusion coëfficient $D_\perp^{exp}$ (Eq. 38) is compared with the classical diffusion coëfficient $D_\perp^{class}$ calculated with (24). The ratio $D_\perp^{exp}/D_\perp^{class}$ is plotted as a function of the electron Hall parameter $\Omega_e \tau_{ei}$. It is observed that for low values of $\Omega_e \tau_{ei}$ indeed the plasma transport is largely reduced as compared with the classical transport, as was previously observed by van der Mullen [13]. Apparently the rotational confinement is quite effective for these values of $\Omega_e \tau_{ei}$. For slightly larger electron Hall parameters (but with ion Hall parameters still below 1) the predictions based on viscosity would indicate even more reduction and even inwardly directed transport.

However, we observe instead a fast deterioration of the rotational confinement and even more transport than classical. Apparently, anomalous diffusion sets in and it is of interest to compare the measured transport with estimates of the anomalous transport based on the measured fluctuation levels of drift- and rotational instabilities. The fluctuation levels of the rotational instability and the drift instability are

Fig. 11. Measured diffusion over classical diffusion as a function of the electron Hall parameter.

shown in Fig. 8 as functions both of $\Omega_e \tau_{ei}$. There is a clear correlation of the level of the drift-waves with the Hall-parameter. For the rotational instability we find a different behaviour: for low values of $\Omega_e \tau_{ei}$ and high values of n_a it is absent, while for the conditions that it is present it saturates at a level of 20% quite independent of the values of the parameters. Estimates of the enhancement of transport by the instabilities are shown in Fig. 11 with an total assumed level of 10% for the rotational instability and including a level of $\tilde{n}_e/n \simeq 3.10^{-4} \Omega_e \tau_{ei}$, (cf. Fig. 8) for the drift instability which are roughly in agreement with the measured levels. We observe that both instabilities together can explain the observed anomalous transport satisfactorily.

As a conclusion we have found that rotational confinement does diminish the transport for low enough values of $\Omega_e \tau_{ei}$ (but still larger than 1). For these conditions the ion-neutral friction and the momentum source terms are the most operative rotational terms. For the condition of our experiment they contribute more to the pressure built up then the Nernst-term. For larger values of $\Omega_e \tau_{ei}$ for which viscosity would dominate rotational confinement, we find instead a deterioration of the confinement and anomalous transport sets in. The observed transport is in agreement with estimates based on the measured fluctuation levels of drift- and rotational instabilities. For still larger values of $\Omega_e \tau_{ei}$ and magnetized ions we expect an influence of rotation on the confinement for conditions with relatively large number of neutrals.

Then the momentum source term will be the most operative. An analysis of the effects of rotation on plasma transport in the outer layers of a Tokamak shows that also there a significant inwardly directed ion flux may result. As discussed in [21] an inwardly directed ion radial velocity of 10 ms^{-1} will result if the rotation velocity of the ions is in the order of 10^4 ms^{-1} (in accordance with estimate a_{0II}) and if the neutral density is 10^{17} m^{-3}. It is therefore of interest to investigate these effects in Tokamaks in more detail making use of recent experimental data of ion poloïdal rotation velocities and neutral densities in the outer layers of a Tokamak.
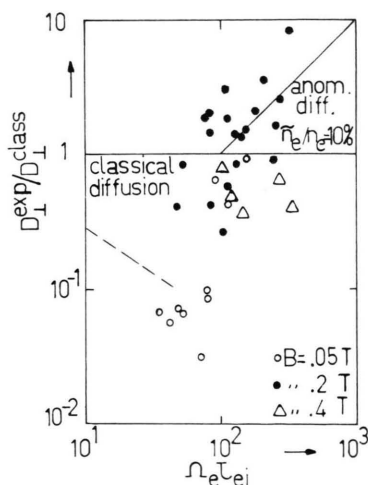
Appendix A

Ordering of the Viscosity- and Friction-Terms in the Ion Momentum Balance

The r- and θ-components of the ion momentum equation in the stationary state and with $\partial/\partial\theta = 0$ are:

r-component:

$$en(E_r + w_{0i}B_z) = nm_i\left[w_{ri}\frac{\partial w_{ri}}{\partial r} - \frac{w_{0i}^2}{r} + w_{zi}\frac{\partial w_{ri}}{\partial z}\right] + \frac{\partial p_i}{\partial r} + en\,w_{zi}B_\theta$$

$$+ (\nabla : \boldsymbol{\Pi}_i)_r + nm_e(w_{ir} - w_{er})/\tau_e + nm_i(w_{ir} - w_{ar})(v_{ia} + v_{ion}). \tag{A-1}$$

θ-component:

$$nm_i\left(\frac{w_{ri}}{r}\frac{\partial}{\partial r}(rw_{0i}) + w_{zi}\frac{\partial w_{0i}}{\partial z}\right) = -en\,w_{ri}B_z - (\nabla \cdot \boldsymbol{\Pi}_i)_\theta + \frac{3}{2}\frac{B_z n}{\Omega_e \tau_e}\frac{\partial kT_e}{\partial r}$$

$$- nm_e(w_{i0} - w_{e0})/\tau_e - nm_i(w_{0i} - w_{0a})(v_{ia} + v_{ion}) \tag{A-2}$$

The r- and θ-components of $(\nabla \cdot \boldsymbol{\Pi}_i)$ are:

$$(\nabla \cdot \boldsymbol{\Pi})_r = -\frac{1}{3}\frac{\partial}{\partial r}\eta_0\left(\frac{\partial w_r}{\partial r} + \frac{w_r}{r} - 2\frac{\partial w_z}{\partial z}\right) - \left[2\eta_1\frac{\partial}{\partial r}\frac{w_r}{r} + \frac{\partial}{\partial r}\eta_1 r\frac{\partial}{\partial r}\frac{w_r}{r}\right]$$

$$-\left[\frac{\partial}{\partial z}\eta_2\frac{\partial w_z}{\partial r} + \frac{\partial}{\partial z}\eta_2\frac{\partial w_r}{\partial z}\right] - \left[2\eta_3\frac{\partial}{\partial r}\frac{w_\theta}{r} + \frac{\partial}{\partial r}\eta_3 r\frac{\partial}{\partial r}\frac{w_\theta}{r}\right] - \frac{\partial}{\partial z}\eta_4\frac{\partial w_\theta}{\partial z}, \tag{A-3}$$

$$(\nabla \cdot \boldsymbol{\Pi})_\theta = -\left[2\eta_1\frac{\partial}{\partial r}\left(\frac{w_\theta}{r}\right) + \frac{\partial}{\partial r}\left(\eta_1 r\frac{\partial}{\partial r}\frac{w_\theta}{r}\right)\right] + \frac{\partial}{\partial z}\left(-\eta_2\frac{\partial w_\theta}{\partial z}\right) + 2\eta_3\frac{\partial}{\partial r}\frac{w_r}{r}$$

$$+ \frac{\partial}{\partial r}\left(\eta_3 r\frac{\partial}{\partial r}\frac{w_r}{r}\right) + \frac{\partial}{\partial z}\left(\eta_4\frac{\partial w_z}{\partial r} + \eta_4\frac{\partial w_r}{\partial r}\right). \tag{A-4}$$

The ion viscosity coefficients are given by:

$$\eta_0 = 0.96\,n_i kT_i \tau_{ii} = 2.02 \cdot 10^{-5}\frac{\hat{T}_i^{5/2}}{\ln\Lambda}, \tag{A-5}$$

and

$$\eta_{1,2,3,4} = n_i kT_i \tau_{ii} f_{1,2,3,4}(\Omega_i \tau_{ii}) \tag{A-6}$$

with (see Fig. A1):

$$f_1 = \frac{4.8\,(\Omega_i \tau_i)^2 + 2.23}{16\,(\Omega_i \tau_i)^4 + 16.1\,(\Omega_i \tau_i)^2 + 2.33},$$

$$f_2 = \frac{1.2\,(\Omega_i \tau_i)^2 + 2.23}{(\Omega_i \tau_i)^4 + 4.03\,(\Omega_i \tau_i)^2 + 2.33},$$

$$f_3 = \frac{8\,(\Omega_i \tau_i)^3 + 4.76\,(\Omega_i \tau_i)}{16\,(\Omega_i \tau_i)^4 + 16.1\,(\Omega_i \tau_i)^2 + 2.33}, \tag{A-7}$$

$$f_4 = \frac{(\Omega_i \tau_i)^3 + 2.38\,(\Omega_i \tau_i)}{(\Omega_i \tau_i)^4 + 4.03\,(\Omega_i \tau_i)^2 + 2.33}.$$

We assume that the ion-velocities can be written as:

$$w_{0i} = a(r)\,r\Omega_i; \quad a(r) = a_0 e^{-r^2/\Lambda_a^2},$$

$$w_{ri} = b(r)\,r\Omega_i; \quad b(r) = b_0 e^{-r^2/\Lambda_b^2}, \tag{A-8}$$

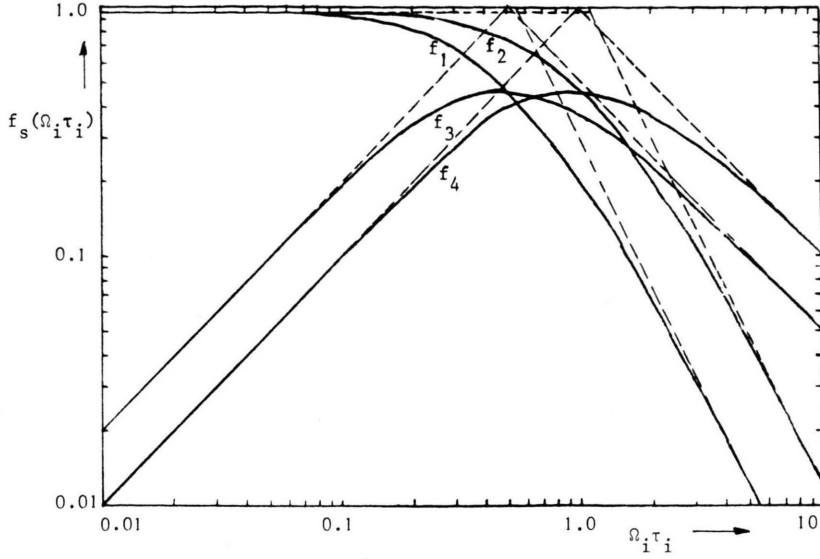$$w_{zi} = c(r)\,v_{thi}, \quad c(r) = c_0 e^{-r^2/\Lambda_c^2}.$$

Fig. A1. Ion-viscosity coefficients as function of the ion Hall parameter $\Omega_i \tau_i$.

The quantities (a_0, b_0, c_0, Λ_a, Λ_b, Λ_c) may still be weak functions of z. Furthermore we assume, that $(w_{0i})_{max} = \alpha \, v_{thi}$, where $\alpha \lesssim 1$. Then we find that

$$a_{0_i} = \alpha \frac{\varrho_{ith}}{\Lambda_a} 2.33 = \xi \frac{\varrho_{ith}}{\Lambda_a} , \quad \text{where } \xi = 2.33 \, \alpha .$$

So for $\alpha \sim 0.5$ we obtain the following estimate for a_0 ((27) with $\xi \sim 1$)

$$a_{0_i} \cong \frac{\varrho_{ith}}{\Lambda_a} , \tag{A-9}$$

where ϱ_{ith} is the thermal ion gyroradius:

$$\varrho_{ith} \equiv \frac{v_{ith}}{\Omega_i} .$$

This estimate has been verified for the unmagnetized ion regime $\Omega_i \tau_{ii} < 1$. Note, that in this regime MHD-ordering requires $\lambda_{ii}/\Lambda \ll 1$ (cf. (4)) but that ϱ_{ith}/Λ may be of the order of 1, as is found in our experiment.

For the magnetized ion regime ($\Omega_i \tau_{ii} > 1$) the second estimate for $a_{0_{II}}$ is relevant. This estimate is based on the assumption that the radial electric field equals roughly the value of the electron temperature in Volt over the radius as indicated in Section 4, cf. (28) − (31):

$$a_{0_{II}} \cong \frac{T_e}{T_i} \frac{\varrho_{ith}^2}{\Lambda^2} . \tag{A-10}$$

In the magnetized ion regime $a_{0_{II}} \ll 1$, as MHD ordering requires here that $\varrho_{ith}/\Lambda \ll 1$ (cf. (4)).

If one assumes classical radial diffusion

$$w_{ri} = \frac{\nabla p_e}{\sigma_\perp B_z^2} \tag{A-11}$$

then we obtain for b_0 the following estimate:

$$b_{0_{cl}} \cong \frac{1}{\Omega_e \tau_{ei}} \left[\frac{T_e}{T_i} \frac{\varrho_{ith}^2}{\Lambda^2} \right] . \tag{A-12}$$

This yields for both regimes a ratio $b_{0_{cl}}/a_0^i \ll 1$. The ratio b_0/a_0 will remain small as compared to unity if the diffusion is anomalously enhanced as observed in our experiment for large values of the electron Hall parameter. If the anomalous diffusion coefficient D^{an} is set equal to $10^{-2} D^{cl} \Omega_e \tau_{ei}$ then $b_{0_{cl}}/a_0 \cong 0.01$ for large values of the electron Hall parameter. The axial component of the ion drift velocity is assumed (and measured) to be smaller than the thermal velocity:

$$c_0 \ll 1 .$$

With these estimates $a_{0_i}(\Omega_i \tau_i < 1)$, $a_{0_{II}}(\Omega_i \tau_i > 1)$, $b_0/a_0 \ll 1$ and $c_0 \ll 1$, ordering of the various terms in (A1, A2) lead to the equations as given in Section 3.

Appendix B

Following the usual notation of collision-radiative models we write for the population densities of the 4p levels in both Ar I and Ar II systems: (only the

equation for the Ar I system is given)

$$n_{\text{rp}} I = r_{4\text{pI}}^{(0)} n_{4\text{pI}}^{\text{Saha}} + r_{4\text{pI}}^{(1)} n_{4\text{pI}}^{\text{Boltzmann}}, \qquad \text{(B-1)}$$

where $n_{4\text{pI}}^{\text{Saha}}$ is the population if the 4p level is in Saha equilibrium with the following ionization stage, whereas $n_{4\text{I}}^{\text{Boltzmann}}$ is the population, if the 4p level is in Boltzmann equilibrium with the ground level of the same system; $r_{4\text{pI}}^{(0)}$ and $r_{4\text{pI}}^{(1)}$ are the so called collisional radiative coefficients. For the parameter range of the experiment we may neglect the "Saha"-contributions. The excitation from the ground state to the 4p-states is mainly balanced by electronic deexcitation to higher levels for both systems. This situation has been called the excitation saturation phase [22]; then the $r^{(1)}$ coefficients are independent on n_e and only weakly dependent on T_e. Furthermore the density of the double ionized state can be neglected, so that $n_i = n_e$. Then we find for the ratio of n_a/n_e:

$$\frac{n_a}{n_e} = \frac{n_{4\text{pI}}}{n_{4\text{pII}}} \frac{g_{4\text{pII}} g_a r_{4\text{pII}}^{(1)}}{g_{4\text{pI}} g_i r_{4\text{pI}}^{(1)}} \exp \frac{E_{4\text{pI}} - E_{4\text{pII}}}{k T_e}. \qquad \text{(B-2)}$$

The collision-radiative coefficients $r_{4\text{pI, II}}^{(1)}$ have to be calculated from collisional radiative models. This is performed in [16] and it appears that (38) can be simplified to:

$$\frac{n_a}{n_e} = C \frac{n_{4\text{pI}} g_{4\text{pII}}}{n_{4\text{pII}} g_{4\text{pI}}} \qquad \text{(B-3)}$$

in which C proves to be approximately constant, independent on n_e and T_e. The magnitude of the constant C can, in principle at least, be determined from Ar I and Ar II CR-models. However, though this procedure does give the correct order of magnitude ($C^{\text{CRM}} \approx 0.06$) it is not very accurate on an absolute scale because of inadequate knowledge of the crucial excitation cross-sections.

We have calibrated C by the use of the relation $p_a(r) = n_a k T_a = \text{constant}$, for the low n_e/n_a, T_e range: $C^{\text{exp}} = 0.11$. The same value for C is obtained from the analysis of the ion energy balance for a much larger parameter range.

[1] C. Mahn, H. Ringler, R. Wienecke, S. Witkowski, and G. Zankl, Z. Naturforsch. **19 a**, 1202 (1964).
[2] H. Wulff, Proc. VIIth ICPIG, Beograd 1965, 829–832.
[3] C. Mahn, H. Ringler, and G. Zankl, Z. Naturforsch. **23 a**, 867 (1968).
[4] K. Bergstedt, Z. Naturforsch. **24 a**, 299 (1969).
[5] P. H. Grassmann, Z. Naturforsch. **23 a**, 251 (1968).
[6] R. Schwenn, Z. Naturforsch. **25 a**, 1310; 1601 (1970).
[7] G. Venus, Z. Physik **259**, 437 (1973).
[8] O. Klüber, Z. Naturforsch. **25 a**, 1583 (1970), part I; **27 a**, 652 (1972), part II.
[9] B. Lehnert, Nuclear Fusion **11**, 485 (1971).
[10] A. van Well, private communication, internal report NT 77-2, Eindhoven University of Technology, 1977.
[11] P. A. E. M. Janssen, Equilibrium and Stability of a Rotating Plasma, Ph. D. thesis, Eindhoven University of Technology (1979). – P. A. E. M. Janssen, F. J. F. van Oldenhoven, Physica **98 c**, 113 (1979).
[12] F. Boeschoten, R. Komen, and A. F. C. Sens, Z. Naturforsch. **34 a**, 1009 (1979).
[13] J. J. A. M. van der Mullen, private communication, internal report NT 78-01, Eindhoven University of Technology (1978). – J. J. A. M. van der Mullen, B. F. M. Pots, D. C. Schram, and B. van der Sijde, Proc. XIVth ICPIG, Grenoble. – J. de Phys. Coll. C7-283 (1979).

[14] S. I. Braginsky and M. A. Leontovich, Reviews of Plasma Physics, Vol. 1, Consultants Bureau, New York 1967.
[15] C. J. Timmermans, A. Lunk, and D. C. Schram, Beitr. Plasma Physik **21**, 117 (1981).
[16] B. F. M. Pots, Turbulence and Transport in a Magnetized Argon Plasma. Ph. D. thesis, Eindhoven University of Technology (1979).
[17] B. F. M. Pots, P. van Hooff, D. C. Schram, and B. van der Sijde, Plasma Physics **23**, 67 (1981).
[18] M. M. B. Wijnakker, E. H. A. Grannema, and J. Kistemaker, Z. Naturforsch. **34 a**, 672 (1979).
[19] B. van der Sijde, Beitr. Plasma Physik **22** (1982), no. 4.
[20] B. F. M. Pots, J. J. H. Coumans, and D. C. Schram, Phys. Fluids **24**, 517 (1981).
[21] D. C. Schram, B. F. M. Pots, and P. A. E. M. Janssen, Proc. 9th Eur. Conf. on Controlled Fusion and Plasma Physics, Oxford 1979, BP 17-71.
[22] J. J. A. M. van der Mullen, B. van der Sijde, and D. C. Schram, Physics Letters **79 A**, 51 (1980).
[23] B. van der Sijde and P. A. W. Tielemans, Proc. 10th ICPIG, Oxford 1971, p. 192.